Hindawi
Advances in Civil Engineering
Volume 2019, Article ID 3689097, 10 pages
https://doi.org/10.1155/2019/3689097

Research Article

Seepage Analysis of a Multilayer Waste Slope considering the Spatial and Temporal Domains of Permeability

Rong Yang,[1] **Zengguang Xu**,[2] **and Junrui Chai**[2]

[1]*Ph.D. Student, State Key Laboratory Base of Eco-hydraulic Engineering in Arid Area, Xi'an University of Technology, Xi'an 710048, China*
[2]*Professor, State Key Laboratory Base of Eco-hydraulic Engineering in Arid Area, Xi'an University of Technology, Xi'an 710048, China*

Correspondence should be addressed to Rong Yang; yangrongxaut123@163.com

Received 9 May 2019; Revised 25 July 2019; Accepted 2 August 2019; Published 25 August 2019

Academic Editor: Giovanni Biondi

Landfilled municipal solid waste has evident heterogeneity, and clogging of the drainage layer can easily happen during operation of the landfill. These two factors significantly influence the distribution of leachate in a landfill. Herein, the distribution of waste permeability in the spatial and temporal domains was analyzed. Then, changes to the drainage-layer permeability in the temporal domain were fitted to these data. A simple model of multilayer waste slope was established combining the finite element software and a user subroutine. Herewith, changes of permeability in the waste and drainage layers were simulated, such that the heterogeneity of waste and the process of clogging of the drainage layer could be simulated. Then, the leachate distributions and transport conditions of nine schemes for landfill were analyzed. The results indicated that the distribution curve of waste-saturated permeability follows a logarithmic relation in the vertical direction, and the distribution curve of fresh-waste-saturated permeability follows a polynomial relation in time. After each landfill is worked for a few years, the drainage layer always encounters clogging problems of some kind and its permeability decreases by one to five orders of magnitude. Through numerical models, the simulation results of the permeability distribution in the spatial and temporal domains were found satisfactory. When the permeability distributions were layered in the buried depth, pore pressures and leachate levels are smaller than the logarithmic distributions. During the process of degradation, the pore pressures and leachate levels are increased slightly under the consideration of the polynomial distribution of waste permeability in time. With clogging of the permeability of the drainage layer, the pore pressures and leachate levels of landfill were found to be increasing gradually. To obtain results closer to that of actual situations, corresponding models should be established and analyzed based on a range of permeability, waste degradation rate, and degree of clogging.

1. Introduction

With the urban development, the output of municipal solid waste (MSW) increases dramatically. The main method for disposal of MSW is landfill. The main problem with landfill is that the leachate level gets too high, which threatens the slope stability of the landfill [1–3]. Thus, it is important to analyze the seepage from landfills. Waste and drainage layer hydraulic conductivities have great effect on the leachate level of a landfill, and they have the characteristics of heterogeneity and unsteadiness.

The factors influencing the waste permeability include their physical composition, content, pressure, density, and particle size distribution [4–8]. Some domestic and overseas experts have studied permeability by both laboratory and field tests [9–13]. Considering operability and cost, laboratory tests are the most commonly used methods to measure permeability. According to statistics, the permeability of landfilled MSW displayed a decreasing trend with the increase of the burying depth. The permeability gradually stabilized in the range of 1.0×10^{-3} m/s to 5.0×10^{-10} m/s [14–16], and the value at the deep end of the landfill is very

small. Due to the MSW being older, the degradation degree is higher, and there is more pressure present at the deep end of the landfill [17]. Based on the laboratory test, field pumping test, formula for forecasting method, and so on, the space distributions of MSW hydraulic conductivity are shown in Figure 1 [18, 19]. Laboratory testing of a landfill was carried out by Jie et al. [20], concluding that the permeability decreases with time and tends to become stable after seven days. By the constant-head test method, the infiltration characteristics of fresh waste with different ratios were studied and the relationships among the permeability, density, and time buried were obtained [17]. These confirmed the results reported by Jie et al. [20]. Wang [21] tested the relationship between permeability of landfill and waste degradation time. The infiltration characteristics of 31 fresh waste samples with high organic contents were then analyzed, and the changes in permeability and density along with compressive strain were determined [22]. This provides a reference for permeability prediction and seepage calculation for similar MSW landfills.

In addition to the distribution of the MSW permeability, the permeability of the drainage layer changes in the temporal domain. In the process of landfill operation, the landfill drainage system will have different degrees of clogging, resulting in a gradual decrease in the permeability coefficient and an increase in the leachate water level. A two-dimensional model was established by Cooke and Rowe [23] to analyze the clogging problem of landfill leachate drainage systems. Through large-scale experimental research, it was found that biological and mineral solids are the causes of drainage pipe clogging [24]. The problem of clogging of the waste drainage layer of different fillers was analyzed through tests by Bazienė et al. [25], and the results indicated that the main substances causing the decrease of permeability were calcium, silicon, and iron compounds. Rowe and Yu [26] analyzed the problem of clogging in landfills by establishing a bioclogging model. Rowe and Yu [27] used the BioClog model to analyze the clogging of landfill leachate flowing through gravel drains. With extended durations of landfill operation, the drain clogs due to physical, chemical, and biological activities [28, 29], that is, the permeability of the drainage layer decreases gradually with waste degradation time. The initial permeability of the drainage layer should not be below 1.0×10^{-3} m/s in China. In terms of testing drainage-layer clogging, the permeability of a landfill in America decreased from 4.2×10^{-4} m/s to 3.1×10^{-8} m/s after six years of operation [30], based on the research data analysis. The study by Bouchez et al. [31] indicated that the main drain clogged by more than 80%. It was shown by statistical analysis that the permeability of drains varied with test methods [32]. After 250–4380 days of operation, the permeability of drainage layer declined by one to two orders of magnitude, with a minimum value of 1.0×10^{-9} m/s.

The leachate level of MSW landfill is very high due to high water content, organic degradation, and rainfall. Generally, the leachate level of landfill form contains main leachate level, perched leachate level, and leachate level of drainage layer. When the drainage layer is clogging, it gathers a large number of leachate and the leachate level of the drainage layer rises to the main leachate level [33]. In terms of field monitoring, pore pressures are measured with an osmometer, and the leachate level and intermediate-layer position are analyzed. Main leachate and perched levels exist in Qizishan landfill, and a 30 cm thick intermediate layer exists at a depth of 10 m [34, 35]. He [36] monitored the leachate level of Xi'an Jiangcungou landfill and established that 2–6 m deep multilayer leachate levels existed in the landfill. In terms of numerical analysis, the seepage of the MSW landfill was simulated by two-dimensional numerical simulation [15, 37, 38]. Qiu et al. [19] studied leachate transport in landfill, considering various rainfall patterns. During the above researches, each layer of waste permeability is simplified into a constant and the variation of the permeability of drainage layer with waste degradation time is not considered. In fact, waste permeability and depth perform the functional relationship and drainage layer is clogging with increasing waste degradation time.

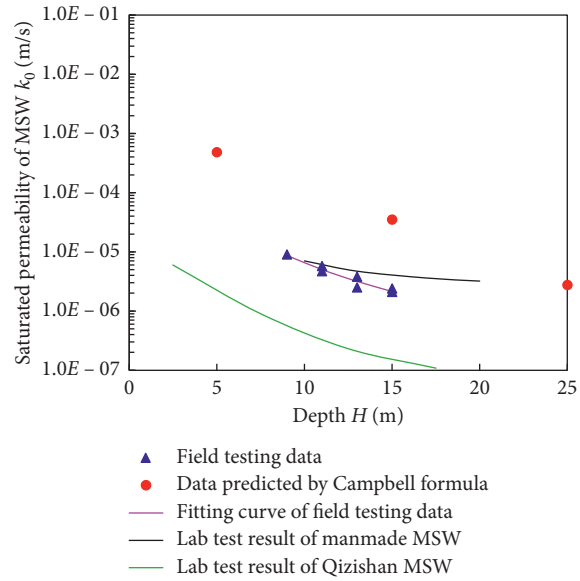

Figure 1: Saturated permeability distribution of Qizishan landfill in the spatial domain [18, 19].

Although the changes to waste infiltration characteristics in the spatial and temporal domains were researched on test, there was relatively less research in numerical calculation, especially regarding the permeability of the waste and drainage layers in the temporal domain. Based on the above research, a method was proposed to simulate changes to the permeability of waste and drainage layers in the spatial and temporal domains. The pore pressures and leachate levels were then analyzed.

2. Permeability Distribution of Landfill

Based on the physical composition, unit weight, and age of MSW, the space and time distribution curves of MSW permeability were gained from relevant references

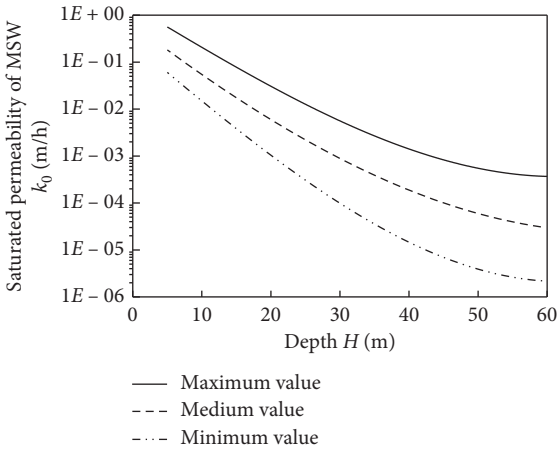

Figure 2: Initial saturated permeability distribution of MSW in the spatial domain [14].

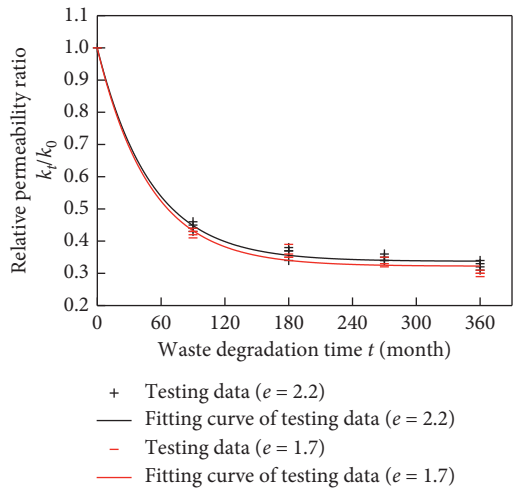

Figure 3: Saturated hydraulic conductivity distribution of MSW in the temporal domain [21].

(Figures 2 and 3) [14, 21]. The initial saturated permeability ranged from 1.0×10^{-3} m/s to 1.0×10^{-10} m/s within 60 m depth, and its rate gradually decreased with the increase of the depth. The relationships between permeability and depth were shown in equations (1)–(3). Based on the permeability test about two different void ratios (e), the relation curves between permeability and waste degradation time are shown in Figure 3 and equations (4) and (5). According to the research by Rowe et al. [38], the permeability of the drainage layer declined from 3.6×10^{-1} m/h to 3.6×10^{-6} m/h in 0–250 d. Three assumptions were made about changes of the permeability of drainage layers, as shown in Figure 4. The medium permeability and void ratio of the waste and similar ranges of permeability of drainage layer, before and after clogging, were analyzed in the manuscript. The permeability distributions of equations (2), (5), and (6) are taken to analyze seepage of landfill:

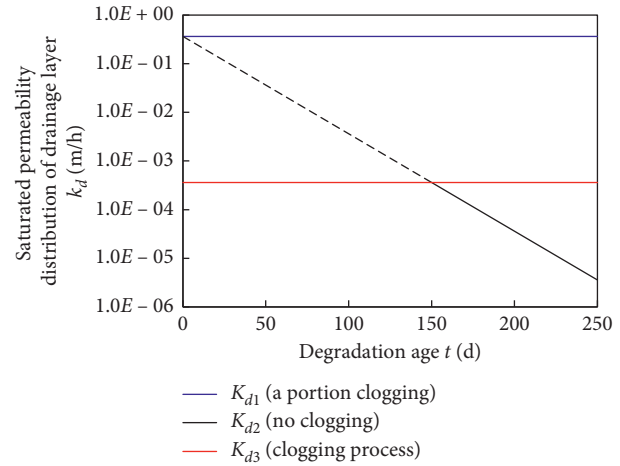

Figure 4: Saturated permeability distribution of drainage layer in the temporal domain [38].

$$\text{minimum value: } \lg k_0 = 3600 \times \left(-4.1589 - 1.2381 \times 10^{-1} H + 3.3109 \times 10^{-5} H^2 + 1.0409 \times 10^{-5} H^3\right), \quad (1)$$

$$\text{medium value: } \lg k_0 = 3600 \times \left(-3.7477 - 1.1207 \times 10^{-1} H + 4.5258 \times 10^{-4} H^2 + 3.5120 \times 10^{-6} H^3\right), \quad (2)$$

$$\text{maximum value: } \lg k_0 = 3600 \times \left(-3.3685 - 8.78 \times 10^{-2} H - 2.5277 \times 10^{-5} H^2 + 8.0405 \times 10^{-6} H^3\right), \quad (3)$$

$$e = 2.2: \frac{k_t}{k_0} = 0.6615 \times e^{(-0.0198t)} + 0.3374, \quad R^2 = 99\%, \quad (4)$$

$$e = 1.7: \frac{k_t}{k_0} = 0.6753 \times e^{(-0.0201t)} + 0.3223, \quad R^2 = 98\%, \quad (5)$$

$$k_{d3} = 3600 \times 10^{-0.012t/24 - 3.997}, \quad t \geq 150\,\text{h}. \quad (6)$$

3. Model and Permeability Simulation

3.1. Calculation Sketch. A multilayer waste slope was selected for simulation. The calculation sketch is shown in Figure 5. The slope ratio is 1 : 3, and the slope height is

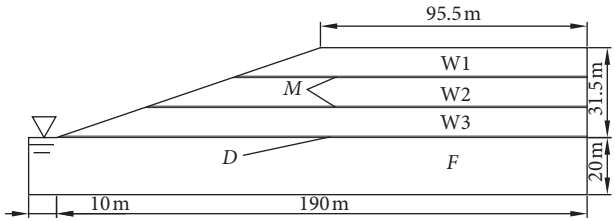

Figure 5: Calculation sketch of the model.

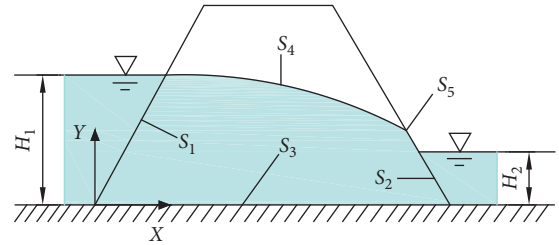

Figure 6: Typical seepage boundary conditions of an earth dam.

31.5 m. The initial ground water is located in the slope toe. $W1$, $W2$, and $W3$ are the waste in the first, second, and third layer, respectively. F indicates the foundation, and M is the middle layer. Here, D is the drainage layer, and its height and initial permeability are 0.5 m and 0.36 m/h, respectively.

3.2. Seepage Theory. The seepage flow-control is shown in the following equation [39]:

$$\frac{\partial}{\partial x}\left(k_x\frac{\partial h}{\partial x}\right)+\frac{\partial}{\partial y}\left(k_y\frac{\partial h}{\partial y}\right)+\frac{\partial}{\partial z}\left(k_z\frac{\partial h}{\partial z}\right)+Q=\frac{\partial \theta}{\partial t}, \quad (7)$$

where k_x, k_y, and k_z are hydraulic conductivities along the x, y, and z directions, respectively; i is the total hydraulic gradient; Q is the water flowing into or out of the soil; t is the time; and θ is the volumetric water content.

The typical seepage boundary conditions of an earth dam can be used for landfill seepage, as shown in Figure 6. The first one is the total head boundary (S_1 and S_2), that is, $\phi_1 = H_1$ and $\phi_2 = H_2$. The second one is the impervious boundary (S_3), and the flux is "0" through the boundary. The third one is the saturated surface (S_4). The position of S_4 is unknown, and the pore pressure is "0". The last one is the free drainage boundary (S_5). The pore pressure is "0," and it can only flow along a downstream slope [40].

3.3. Numerical Model and Permeability Simulation. According to Figure 5, a model was established using ABAQUS/Standard software (Figure 7) and the parameters for each part of the material were set in the model (Table 1). It was assumed that the landfill volume does not change during computing and that the permeabilities of the waste and drainage layers change as follows. Permeability of MSW layers distributed in depth is shown in Figure 8.

The permeability distributions in the spatial and temporal domains were defined using the USDFLD subroutine of ABAQUS software [40, 41]. The simulation steps are as follows:

(1) The finite element model was established using ABAQUS, and the grid was divided. The material properties were then set, the keywords of waste or drainage layer saturated permeability were edited, and the field variables related to permeability were defined.

(2) The relationships among the field variable, Y coordinate, and t were defined by the USDFLD user subroutine to determine the permeability distribution of a landfill in the spatial and temporal domains.

(3) The time step and initial conditions were set, and the boundary constraint and load were applied.

(4) Variable outputs were defined for FV1 and FV2. FV1 refers to the permeability of MSW in a logarithmic distribution in the spatial domain, and FV2 refers to the permeability of MSW distributed logarithmically and indexed in the spatial and temporal domains. The calculation results exhibited the field variable distributions, namely, the permeability distribution (see Figures 9 and 10). The distributions of characteristics in the spatial and temporal domains are simulated in Figure 10 based on the Z-zone of the model in Figure 9.

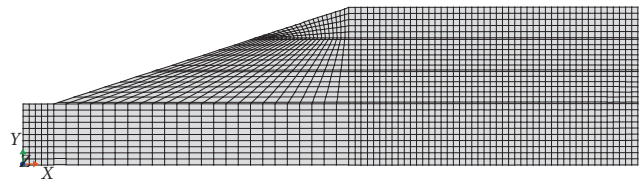

Figure 7: Mesh of the finite element model.

3.4. Calculation Scheme Design. Considering the permeability distributions of the waste and drainage layers in the spatial and temporal domains, the influence of permeability variations on the seepage field were studied. The following nine schemes were adopted for analysis (Table 2). The effects of k_{wa} and k_{d1} are considered in Scheme 1; the effects of k_{wa} and k_{d2} are considered in Scheme 4, and they are suitable for seepage analysis of low landfill in the short term. Schemes 2 and 5 are suitable for seepage analysis of high landfill in the short term. Schemes 3 and 6 are suitable for seepage analysis of high landfill in the long term. Schemes 7, 8, and 9 are suitable for seepage analysis of landfill in the long term, due to drainage clogging. The mesh was the same for all of the schemes in the models. The intensity of rainfall infiltration was 0.02 m/h at the top of the landfill slope and was converted in the slope, based on the ratio of the slope. The rainfall pattern was the center type. The amplitude curve of the rainfall intensity is shown in Figure 11. The initial groundwater level was 20 m. The drainage-only flow of the slope was set, and the variation of pore pressure was calculated and analyzed.

Table 1: Parameters of each part of the material.

Material (the vertical coordinate Y)	Consideration	Symbol of permeability	Permeability (m/h)
$W1$ ($20.5\,\text{m} < Y \le 30.5\,\text{m}$)	Layering distribution	k_{wa}	0.0021
	Function distribution in the spatial domain	k_{wb}	Equation (2)
	Function distribution in the spatial and temporal domains	k_{wc}	Equations (2) and (5)
$W2$ ($31.0\,\text{m} < Y \le 41.0\,\text{m}$)	Layering distribution	k_{wa}	0.017
	Function distribution in the spatial domain	k_{wb}	Equation (2)
	Function distribution in the spatial and temporal domains	k_{wc}	Equations (2) and (5)
$W3$ ($41.5\,\text{m} < Y \le 51.5\,\text{m}$)	Layering distribution	k_{wa}	0.18
	Function distribution in the spatial domain	k_{wb}	Equation (2)
	Function distribution in the spatial and temporal domains	k_{wc}	Equations (2) and (5)
D ($20.0\,\text{m} < Y \le 20.5\,\text{m}$)	A portion clogging	k_{d1}	0.00036
	No clogging	k_{d2}	0.36
	Considering the clogging process	k_{d3}	Equation (6)
M ($30.5\,\text{m} < Y \le 31.0\,\text{m}$) ($41.0\,\text{m} < Y \le 41.5\,\text{m}$)	—		3.6×10^{-4}
F ($0\,\text{m} < Y \le 20.0\,\text{m}$)	—		3.6×10^{-4}

where k_{wa}, k_{wb}, and k_{wc} are saturated permeability distributions of waste under three assumptions at moment t (m/h); k_d is the saturated permeability of the drainage layer (m/h); t is the time (h); and Y is the vertical coordinate value (m).

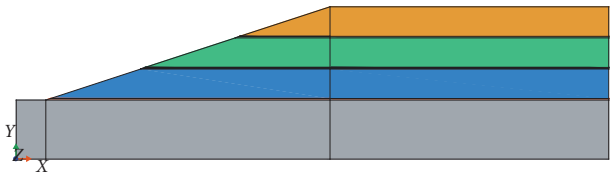

Figure 8: Permeability of MSW layers distributed in the spatial domain.

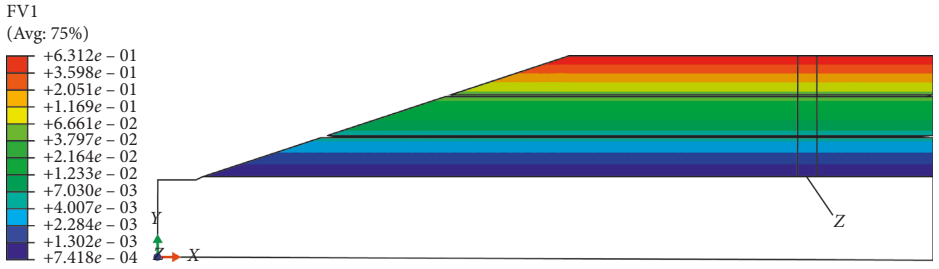

Figure 9: Permeability of MSW in a logarithmic distribution in the spatial domain (m/h).

4. Results and Discussion

In order to compare and analyze the results of all schemes, several key positions are selected and analyzed in Figure 12. The location of $L1$ is $X = 106$ m, and the coordinates of P1, P2, P3, P4, and P5 are (51, 33), (116, 22), (116, 33), (116, 44), and (116, 50), respectively. The seepage field was analyzed based on the pore pressure and leachate level.

4.1. Pore Pressure. In this landfill structure, the permeability of the waste was distributed as layers (Scheme 1) and function (Scheme 2) in the vertical direction, and the calculation results were compared and analyzed. The distributions of pore pressure of $L1$ in both schemes are shown in Figures 13 and 14. When pore pressure was greater than 0 kPa, leachate exists in the landfill. The leachate levels included surface, perched, and main leachate levels. The pore pressure varied from −320 kPa to 280 kPa. In Scheme 1, there were one main and two perched leachate levels in the landfill. The shallow waste permeability had the larger constant and the permeability of the middle layer decreased clearly as an evident change occurred in the pore pressure at the middle layer. Thus, visible interception of rainfall occurred. In Scheme 2, there was a main and a surface leachate level in the landfill during rainfall. Due to gradual decrease of the waste permeability with depth, the rate of rainfall infiltration decreased, and the leachate level appeared in the surface waste. A comparison shows that the pore pressures of the waste pile (20–40 m depth) in Scheme 2 was greater

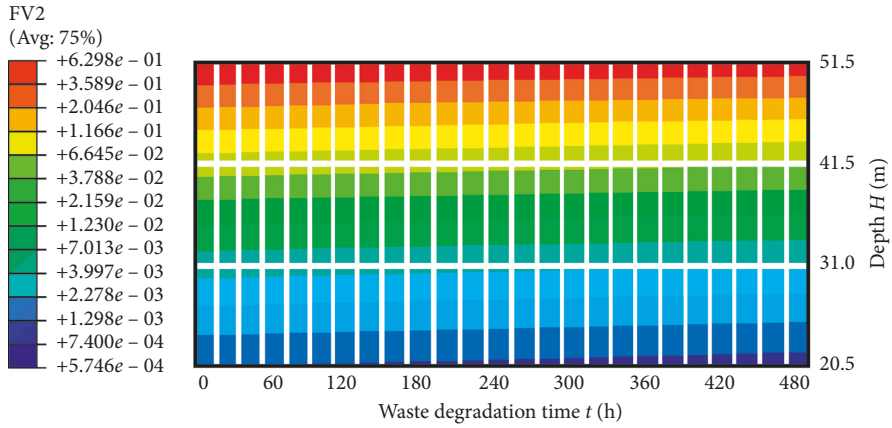

Figure 10: Permeability of MSW distributed logarithmically and indexed in the spatial and temporal domains, respectively (m/h).

Table 2: Calculation schemes.

Scheme		Permeability of drainage layer (m/h)		
		k_{d1} ↓	k_{d2}	k_{d3}
Permeability of MSW (m/h)	k_{wa} ⟶	Scheme 1	Scheme 4	Scheme 7
	k_{wb}	Scheme 2	Scheme 5	Scheme 8
	k_{wc}	Scheme 3	Scheme 6	Scheme 9

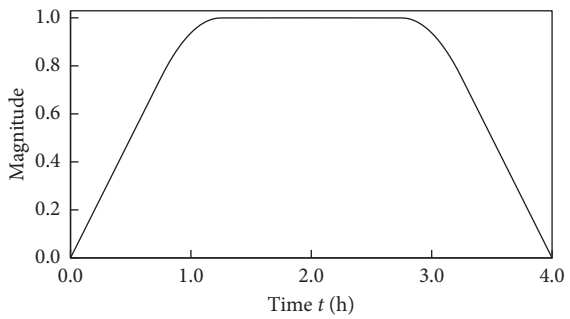

Figure 11: Amplitude curve of rainfall intensity.

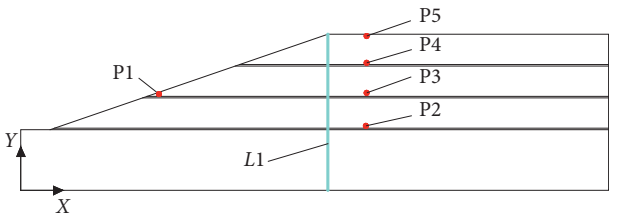

Figure 12: Distribution graph of key positions.

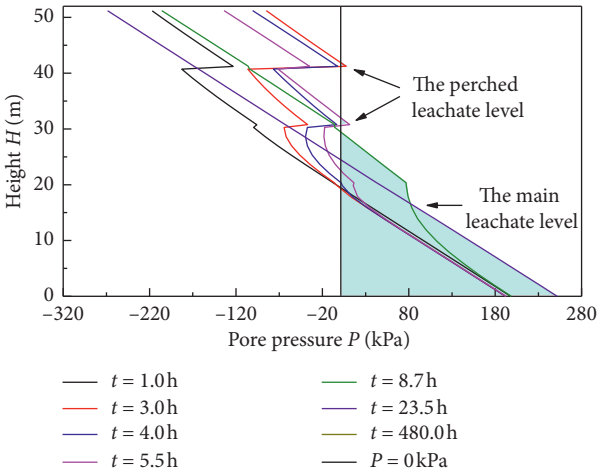

Figure 13: Vertical distribution curve of pore pressure at $L1$ in Scheme 1.

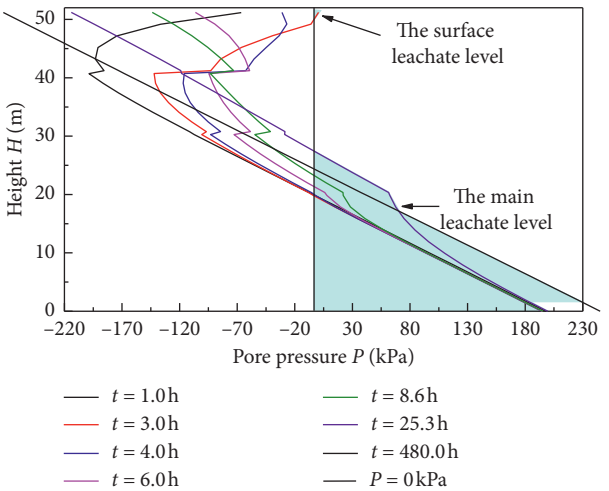

Figure 14: Vertical distribution curve of pore pressure at $L1$ in Scheme 2.

than that in Scheme 1. Similarly, the pore pressure distribution in Schemes 4 and 5 was basically the same and also in Schemes 7 and 8.

The permeability of the waste was distributed as a constant (Scheme 2) and function (Scheme 3) in time. Table 3 displays the pore pressure distribution in both the schemes. Taking observation points from P2 to P5, it can be seen that the pore pressure of Scheme 3 is larger than that of

Table 3: Variation of pore pressure at P2–P5 with time in Scheme 2 and Scheme 3.

Time t (day)	Pore pressure P (kpa)							
	Scheme 2				Scheme 3			
	P2	P3	P4	P5	P2	P3	P4	P5
1	−9.12	−8.90	−7.75	−24.43	−9.09	−8.76	−7.74	−24.42
3	+2.05	+0.27	−10.98	−27.38	+2.06	+0.06	−10.97	−27.35
4	−5.90	−26.58	−8.94	−25.01	−5.87	−26.46	−8.86	−24.92
6	−38.47	−88.15	+2.46	−12.75	−38.41	−87.88	+2.72	−12.46
10	−56.77	−122.17	+29.48	+15.08	−56.70	−121.78	+29.91	+15.52
25	−71.75	−145.27	+63.47	+48.33	−71.62	−144.86	+63.78	+48.64
480	−91.42	−178.54	+37.34	+20.62	−91.35	−178.47	+37.39	+20.67

Scheme 2. At the beginning of the rain, the pore pressure at P2 and P3 are less affected by rainfall due to middle-layer interception. In both the schemes, the change in trend of pore pressure is consistent; the pore pressure increases first and then decreases gradually. Comparing the two schemes, the pore pressure is slightly larger because the waste permeability in Scheme 3 decreases with time.

When the spatial distribution of the waste permeability and the drainage layer clogging are considered, Figures 15 and 16 depict the pore pressure distributions at P1 and P3 at the same depth over time. The pore pressure distributions in Schemes 1 and 4 are basically the same during the rain, and the same is true for Schemes 2 and 5. The pore pressure order at P1 and P3 is Scheme $1 > 2 > 4 > 5$. Through analysis, the permeability of drainage layer decreases and then the pore pressure of the landfill increases after drainage layer clogging (such as Schemes 1 and 2). When the permeability of the waste is distributed as a function in the vertical direction, the pore pressure of the landfill is lower and it dissipates faster (such as Schemes 2 and 5). At the point of slope P1, the seepage is mainly influenced by the drainage layer. Thus, the pore pressures of Schemes 1 and 2 are larger at the early stage. On the contrary, the seepage is mainly influenced by the permeability distribution of waste at the point P3. Thus, the pore pressures of Schemes 1 and 4 are larger at the early stage.

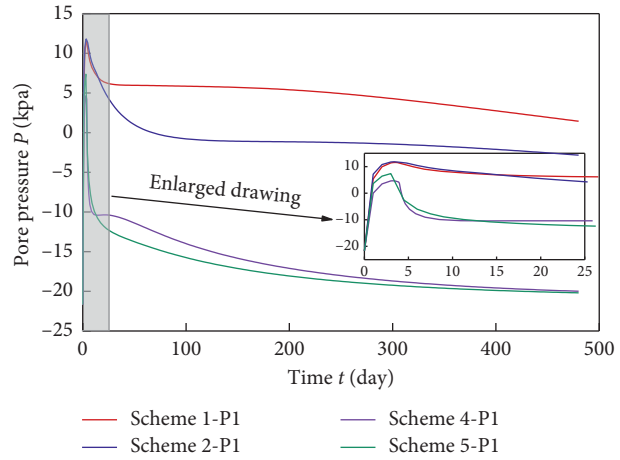

Figure 15: Variation curves of the pore pressure at P1 with time in four schemes.

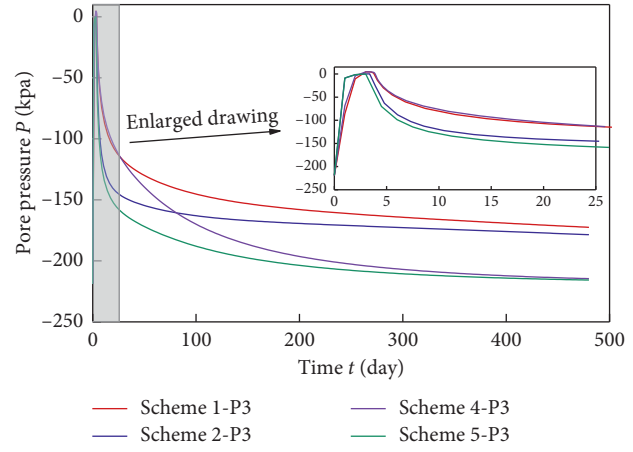

Figure 16: Variation curves of pore pressure at P3 with time in four schemes.

4.2. Leachate Level. At the end of the rain ($t = 4$ h), Figures 17 and 18 show the leachate level distributions in Schemes 1 and 2. It can be seen directly that the distribution type of the waste permeability has a greater influence on leachate level in landfills. In Scheme 1, the leachate level in the slope is higher and two perched leachate levels exist. In Scheme 2, there is only one perched leachate level in the slope and there is a higher surface leachate level at the top of the landfill. This is because when considering the distribution of waste permeability as layers, the permeability of the middle layer suddenly decreases, which makes it easy to retain leachate.

The distributions of leachate level $L1$ in several schemes are shown in Figure 19 within 25 h, and the positions of the leachate level are marked. When the time is 3 h, the surface leachate levels exist in Schemes 2, 5, and 8. Perched leachate levels at 3 h exist in Schemes 1, 4, and 7. When the time is 25 h, the leachate level order of the six schemes is Scheme $7 > 1 > 4 > 8 > 2 > 5$. The leachate levels of these schemes are shown in Figure 20 ($t = 25$–480 h) and Table 4 ($t = 480$ h). It can be seen that the leachate level in Scheme 7 is the highest and the leachate level in Scheme 2 is the lowest. When the permeability of the drainage layer is 0.36 m/h, the leachate is discharged quickly. The leachate level of slope is near the underground water level with a value of 20.048 m. When the time is 480 h, the permeability of the drainage layer in

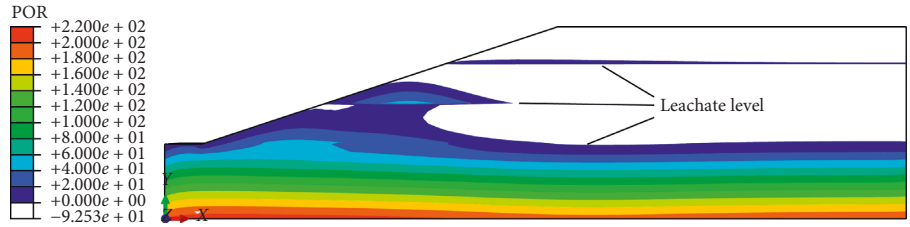

Figure 17: Leachate level in Scheme 1 ($t = 4$ h).

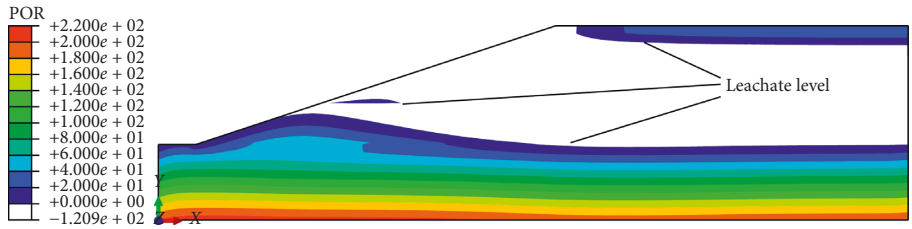

Figure 18: Leachate level in Scheme 2 ($t = 4$ h).

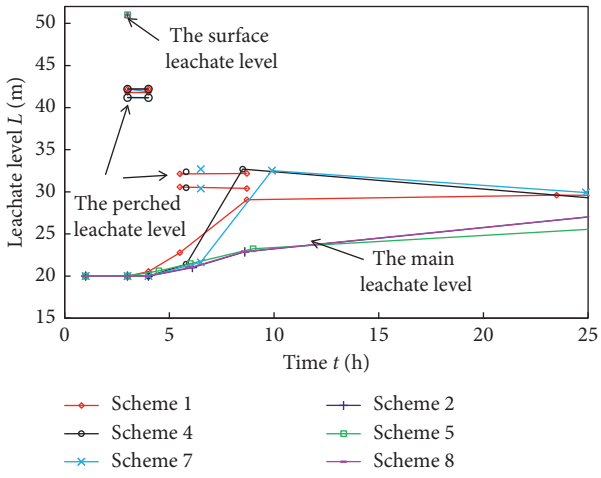

Figure 19: Leachate level distributions of several schemes ($t = 0$–25 h).

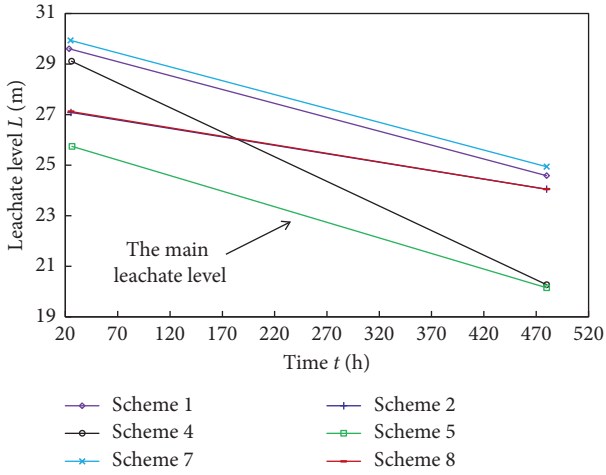

Figure 20: Leachate level distributions of several schemes ($t = 25$–480 h).

Table 4: Leachate levels of all schemes ($t = 480$ h).

Scheme	1	2	4	5	7	8
Leachate level (m)	24.584	24.048	20.269	20.153	24.943	24.053

Scheme 7 is the least in all of the schemes and the waste permeability is distributed as layers. In this case, the leachate infiltration is relatively slow and eventually the leachate level is the highest. The leachate level order of the six schemes is Scheme $7 > 1 > 4 > 5 > 8 > 2$. In conclusion, when considering the distribution of waste permeability as layers, the perched leachate level is readily produced in the landfill at the beginning of a rain although leachate infiltration has a lag. Eventually, the leachate level is relatively high. When considering the distribution of waste permeability as a function, the surface leachate level is easily produced in the landfill at the beginning of a rain. The leachate moves down gradually, and eventually, a perched leachate level is produced.

5. Conclusions

Considering the heterogeneity of landfilled waste and drainage layer clogging, the distributions of waste permeability in the spatial and temporal domains and the changes to drainage layer permeability in the temporal domain were analyzed. Then, by combining finite element software and a user subroutine, a simple model of a landfill was established and the permeability of the waste and drainage layers was simulated. Finally, the leachate distributions and transport conditions of the landfill were analyzed, and the influence of the distribution of waste permeability and the degree of the drainage layer clogging was discussed. The main conclusions of the study are as follows:

(i) The value of saturated permeability of the landfill ranged from 1.0×10^{-4} m/s to 1.0×10^{-9} m/s, and it

followed a logarithmic relationship vertically. The saturated permeability of the waste distribution curve followed an exponential relation in time. After the landfill was worked for a few years, the drainage layer always exhibited some form of a clogging problem and its permeability decreased by one to five orders of magnitude.

(ii) The simulation method of saturated permeability of the landfill in the spatial and temporal domains was studied. It was possible to simulate the distribution of saturated permeability by a variety of functions, and the results were satisfactory. In addition, this method could be used for the consolidation of sand drains, tailing dam siltation, and other geotechnical engineering conditions.

(iii) At the same clogging degrees of the drainage layer, the overall pore pressure was relatively large considering the distributions of waste permeability as layers (vertically). An evident change occurred in the pore pressure at the middle layer, which assisted a perched leachate level to occur at the top of the landfill. Considering the distributions of waste permeability as a vertical logarithmic relationship, the surface leachate level was produced first; then, the leachate moved down and produced a lower perched leachate level.

(iv) At the same clogging degrees of the drainage layer, the variational trends were the same and the influence of the waste permeability distribution on the pore pressure at the top of the landfill was greater than that of the pore pressure at the bottom of the landfill, irrespective of consideration of the polynomial relation of waste permeability in time.

(v) When the distributions of waste permeability were the same and the clogging problem occurred in the drainage layer, the change in pore pressure over time was essentially the same during the rain; the pore pressure dissipation was slower and the leachate level was higher.

In conclusion, corresponding models should be established and analyzed based on the permeability range, waste degradation rate, and the degree of clogging in order to make the results converge to that of actual situations.

Data Availability

The data used to support the findings of this study are available from the corresponding author upon request.

Conflicts of Interest

The authors declare that there are no conflicts of interest regarding the publication of this paper.

Acknowledgments

This study was financially supported by the National Natural Science Foundation of China (51679193 and 51679197) and the Special Funds for the Natural Science Foundation of Shaanxi Province (2017JZ013). We thank LetPub (https://www.letpub.com) for its linguistic assistance during the preparation of this manuscript.

References

[1] B. Caicedo, E. Giraldo, and L. Yamin, "The landslide of dona juana landfill in bogota. A case study," in *Proceedings of the Fourth International Congress on Environmental Geotechnics (4th ICEG)*, pp. 11–15, Rio de Janeiro, Brazil, August 2002.

[2] R. G. Koerner and W. A. Eith, *Drainage Capability of Fully Degraded MSW with Respect to Various Leachate Collection and Removal Systems*, Geotechnical Special Publication, Denver, CO, USA, 2005.

[3] S. M. Merry, E. Kavazanjian Jr., and W. U. Fritz, "Reconnaissance of the july 10, 2000, payatas landfill failure," *Journal of Performance of Constructed Facilities*, vol. 19, no. 2, pp. 100–107, 2005.

[4] Y. Chen, X. Xu, and L. Zhan, "Analysis of solid-liquid-gas interactions in landfilled municipal solid waste by a bio-hydro-mechanical coupled model," *Science China Technological Sciences*, vol. 55, no. 1, pp. 81–89, 2012.

[5] X. B. Xu, T. L. T. Zhan, Y. M. Chen, and R. P. Beaven, "Intrinsic and relative permeabilities of shredded municipal solid wastes from the Qizishan landfill, China," *Canadian Geotechnical Journal*, vol. 51, no. 11, pp. 1243–1252, 2014.

[6] M. Y. Li, H. K. Jae, and Q. Y. Xu, "Review about hydraulic conductivity of landfilled waste," *Environmental Engineering*, vol. 8, pp. 80–84, 2014.

[7] S. Gavelyte, E. Dace, and K. Baziene, "The effect of particle size distribution on hydraulic permeability in a waste mass," *Energy Procedia*, vol. 95, pp. 140–144, 2016.

[8] Z. Zhang, Y. Wang, H. Xu, Y. Fang, and D. Wu, "Influence of effective stress and dry density on the permeability of municipal solid waste," *Waste Management & Research*, vol. 36, no. 5, pp. 471–450, Article ID: 734242X18763520, 2018.

[9] F. Olivier and J.-P. Gourc, "Hydro-mechanical behavior of municipal solid waste subject to leachate recirculation in a large-scale compression reactor cell," *Waste Management*, vol. 27, no. 1, pp. 44–58, 2007.

[10] K. R. Reddy, H. Hettiarachchi, N. Parakalla, J. Gangathulasi, J. Bogner, and T. Lagier, "Hydraulic conductivity of MSW in landfills," *Journal of Environmental Engineering*, vol. 135, no. 8, pp. 677–683, 2009.

[11] M. S. Hossain, K. K. Penmethsa, and L. Hoyos, "Permeability of municipal solid waste in bioreactor landfill with degradation," *Geotechnical and Geological Engineering*, vol. 27, no. 1, pp. 43–51, 2009.

[12] G. Stoltz, J.-P. Gourc, and L. Oxarango, "Liquid and gas permeabilities of unsaturated municipal solid waste under compression," *Journal of Contaminant Hydrology*, vol. 118, no. 1-2, pp. 27–42, 2010.

[13] H. Wu, T. Chen, H. Wang, and W. Lu, "Field air permeability and hydraulic conductivity of landfilled municipal solid waste in China," *Journal of Environmental Management*, vol. 98, pp. 15–22, 2012.

[14] Ministry of Housing and Urban-Rural Development of the People's Republic of China 2012, *Technical Code for Geotechnical Engineering of Municipal Solid Waste Sanitary Landfill, CJJ176-2012*, China Construction Industry Press, Beijing, China, 2012.

[15] R. Yang, Z. Xu, J. Chai, Y. Qin, and Y. Li, "Permeability test and slope stability analysis of municipal solid waste in

Jiangcungou Landfill, Shaanxi, China," *Journal of the Air & Waste Management Association*, vol. 66, no. 7, pp. 655–662, 2016.

[16] R. Yang, Z. Xu, and J. Chai, "A review of characteristics of landfilled municipal solid waste in several countries: physical composition, unit weight, and permeability coefficient," *Polish Journal of Environmental Studies*, vol. 27, no. 6, pp. 2425–2435, 2018.

[17] Z. Y. Zhang, L. F. Zhang, D. Z. Wu et al., "Experimental study on permeability of fresh municipal solid waste with different mixed proportion," *Journal of Zhejiang Sci-Tech University (Natural Sciences)*, vol. 35, no. 5, pp. 796–802, 2016.

[18] Z. Liu, "*Experimental study on hydraulic conductivity of municipal solid waste and analysis of pumping vertical well*," M.S. thesis, Zhejiang University, Hangzhou, China, 2010.

[19] Z. H. Qiu, C. M. He, B. J. Zhu et al., "Investigations of water transport in valley-type MSW landfills and their stabilities subjected to various rainfall patterns," *Rock and Soil Mechnics*, vol. 33, no. 10, pp. 3151–3170, 2012.

[20] Y. X. Jie, D. Z. Danzeng, and Y. F. Wei, "Study on the permeability of municipal solid waste," *Geotechnical Engineering Technique*, vol. 19, no. 6, pp. 307–310, 2005.

[21] W. F. Wang, "Laboratory research on saturated hydraulic conductivity of municipal solid waste under different degradation age," Master's degree thesis, Zhejiang University, Hangzhou, China, 2012.

[22] Z. Y. Zhang, Z. K. Ding, Y. F. Wang, D. Z. Wu, and Z. P. Zhang, "Experimental study on the compression and permeability combined test of fresh municipal solid waste with higher organic matter," *Chinese Journal of Rock Mechanics and Engineering*, no. S1, pp. 3645–3651, 2018.

[23] A. J. Cooke and R. K. Rowe, "2D modelling of clogging in landfill leachate collection systems," *Canadian Geotechnical Journal*, vol. 45, no. 10, pp. 1393–1409, 2008.

[24] S. Lozecznik and J. Van Gulck, "Full-scale laboratory study into clogging of pipes permeated with landfill leachate," *Practice Periodical of Hazardous Toxic & Radioactive Waste Management*, vol. 13, no. 4, pp. 261–269, 2009.

[25] K. Bazienė, S. Vasarevičius, and A. A. Siddiqui, "Clogging test of landfill leachate drainage using different fillers," *Journal of Environmental Engineering and Landscape Management*, vol. 20, no. 4, pp. 301–306, 2012.

[26] R. K. Rowe and Y. Yu, "Clogging of finger drain systems in MSW landfills," *Waste Management*, vol. 32, no. 12, pp. 2342–2352, 2012.

[27] R. K. Rowe and Y. Yu, "Modelling of leachate characteristics and clogging of gravel drainage mesocosms permeated with landfill leachate," *Journal of Geotechnical and Geoenvironmental Engineering*, vol. 139, no. 9, pp. 1022–1034, 2012.

[28] Q. Tang, F. Gu, Y. Zhang, Y. Zhang, and J. Mo, "Impact of biological clogging on the barrier performance of landfill liners," *Journal of Environmental Management*, vol. 222, pp. 44–53, 2018.

[29] Z. Li, Q. Xue, L. Liu, and J. Li, "Precipitates in landfill leachate mediated by dissolved organic matters," *Journal of Hazardous Materials*, vol. 287, pp. 278–286, 2015.

[30] R. M. Koerner and G. R. Koerner, *Leachate Clogging Assessment of Geotextile (And Soil) Landfill Filters*, US Environmental Protection, Washington, DC, USA, 1995.

[31] T. Bouchez, M. L. Munoz, S. Vessigaud, C. Bordier, and C. Aran, "Clogging of MSW landfill leachate collection systems: prediction methods and in situ diagnosis," in *Proceedings of the 9th International Waste Management and Landfill Symposium*, Cagliari, Italy, October 2003.

[32] Y. M. Chen, J. W. Lan, Y. C. Li, L. T. Zhan, and H. Ke, "Development and control of leachate mound in MSW landfills," *Chinese Journal of Rock Mechanics and Engineering*, vol. 33, no. 1, pp. 154–163, 2014.

[33] Z. G. Xu, R. Yang, and X. M. Yang, *"Research on Special Geotechnical Hydraulic Conductivity—Taking Tailings Dam and MSW Landfill as Examples*, Science Press, Beijing, China, 2016.

[34] W. J. Zhang, W. A. Lin, and Y. M. Chen, "Pore pressure monitoring and slope stability analysis of a waste landfill," *Chinese Journal of Rock Mechanics and Engineering*, vol. 29, no. S2, pp. 3628–3632, 2010.

[35] W.-J. Zhang, G.-G. Zhang, and Y.-M. Chen, "Analyses on a high leachate mound in a landfill of municipal solid waste in China," *Environmental Earth Sciences*, vol. 70, no. 4, pp. 1747–1752, 2013.

[36] H. J. He, "Study on leachate and landfill gas generation, transportation and induced slope instability in municipal solid waste landfill," Doctor's degree thesis, Zhejiang University, Hangzhou, China, 2012.

[37] W. J. Zhang, "Experimental and numerical study on water/leachate transport in landfill of municipal solid waste," Doctor's degree thesis, Zhejiang University, Hangzhou, China, 2007.

[38] R. K. Rowe, M. D. Armstrong, and D. R. Cullimore, "Mass loading and the rate of clogging due to municipal solid waste leachate," *Canadian Geotechnical Journal*, vol. 37, no. 2, pp. 355–370, 2000.

[39] C. X. Mao, *Seepage Calculation Analysis and Control*, China Water Resources and Hydropower Press, Beijing, China, 2003.

[40] Abaqus 6.14, User subroutines reference guide, Section 1.1.7 (1–3), Section 1.1.32 (1–4).

[41] K. Fei and J. W. Zhang, *Abaqus Application in Geotechnical Engineering*, China Water Resources and Hydropower Press, Beijing, China, 2009.